

# ARTICLE

## Portable and Sustainable Device for Arsenic and Lead Water Purification

Received 00th January 20xx,  
Accepted 00th January 20xx

Tomer Noyhouzer,<sup>a</sup> Nicholas A. Payne,<sup>a</sup> Siba Moussa,<sup>a</sup> Isabelle Beaulieu,<sup>a</sup> and Janine Mauzeroll<sup>\*</sup>

DOI: 10.1039/x0xx00000x

### Supplementary Information

**Table S1:** Heavy metals removal efficiency. The volume represents the total treated volume during this experiment. Each solution contained 1 M HCl spiked with 1 ppm of As and Pb. The confidence level was calculated based on a standard deviation (95%) of 5 repeats.

	Electroless Filtration 70 mL	Constant Potential (-1 V) Filtration 70 mL	Constant Potential (-1 V) 280 mL
<b>As</b>	6 ±2 %	29±2 %	20±2
<b>Pb</b>	32±2%	55±3 %	39±2

**Table S2:** Comparison of the removal efficiencies after the PoWPU was treated with different regeneration solvents with and without (electroless) applied voltage (+1 V). The confidence level was calculated based on a standard deviation (95%) of 5 repeats.

	Without Applied Voltage			With Applied Voltage		
	Acetic Acid 5%	Nitric Acid 5%	HCl 1 M	Acetic Acid 5%	Nitric Acid 5%	HCl 1 M
<b>As</b>	11 ±3 %	21±1 %	19±2 %	55±4 %	81±2 %	65±2 %
<b>Pb</b>	12±3 %	21±1 %	24±2 %	40±3 %	61±1 %	64±2 %

**Table S3:** Comparison of the removal efficiencies between the different results after passing 70 mL of 1 ppm As and Pb solution through the system. The confidence level was calculated based on a standard deviation (95%) of 5 repeats.

	Electroless Filtration 1M HCl	Coulometric Filtration 1M HCl	Coulometric Filtration pH 5.5	Coulometric Filtration Tap Water
<b>As</b>	6 ±2 %	29 ±1 %	68 ±2 %	38.5 ±3 %
<b>Pb</b>	32 ±2 %	55 ±3 %	79 ±3 %	47.5 ±2 %

<sup>a</sup> Department of Chemistry, McGill University, 801 Sherbrooke West, Montreal, QC, Canada H3A 0B8. E-mail: janine.mauzeroll@mcgill.ca

**Table S4:** Comparison between different methods used to improve the regeneration of As and Pb using tap water. Each solution contained 1 M HCl spiked with 1 ppm of As and Pb. The confidence level was calculated based on a standard deviation (95%) of 5 repeats.

	Electroless	Constant Potential (1 V)	Pulsing Potential (1 to -1 V)
As	42 ± 2 %	98 ± 3 %	99 ± 3 %
Pb	58 ± 2 %	79 ± 1 %	97 ± 2 %

**Table S5:** Relevant reactions that occurs on the CE with standard potentials or acid dissociation constants.<sup>1</sup>

	Reaction	E° vs NHE / K <sub>a</sub>
As	$H_3AsO_3 + H_2O \rightleftharpoons H_3AsO_4(aq) + 2H^+ + 2e^-$	E° = 0.234 V
	$H_3AsO_4(aq) \rightleftharpoons H_2AsO_4(aq) + H^+$	K <sub>a</sub> = 5.98 × 10 <sup>-3</sup>
	$H_2AsO_4(aq) \rightleftharpoons HAsO_4(aq) + H^+$	K <sub>a</sub> = 1.04 × 10 <sup>-7</sup>
Pb	$Pb^{2+} + 2H_2O \rightleftharpoons PbO_{2(s)} + H^+ + 2e^-$	1.46 V

**Table S6:** The change of the filtration efficiency as a function of the flow rate. Each solution contained 1 M HCl spiked with 1 ppm of As and Pb. The confidence level was calculated based on a standard deviation (95%) of 3 repeats.

Flow rate (mL S <sup>-1</sup> )	1	5	10
As	78 ± 7 %	53 ± 8 %	27 ± 7 %
Pb	59 ± 8 %	32 ± 5 %	14 ± 4 %

The PoWFU syringe design (Figure 1B, Figure S1) consists of two GAC packed electrodes separated by a thin layer of polyurethane foam used as both a separator and porous plug. The presence of the reference electrode was required for laboratory testing but was removed in the final device.

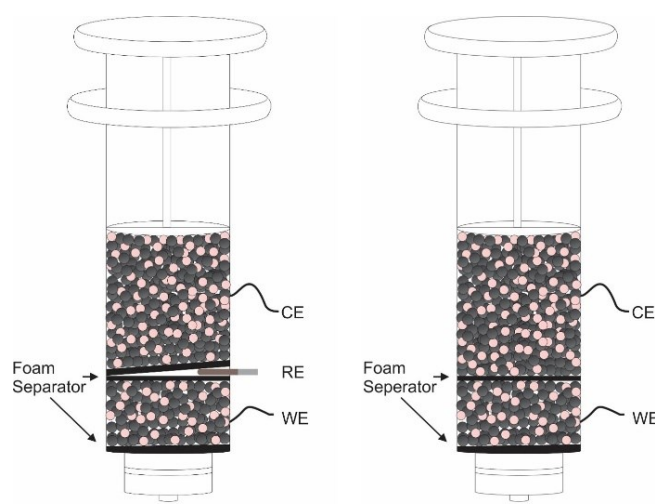


**Figure S1:** The two cell designs that were used with a QRE Ag/AgCl reference electrode (left) and without (right). The electrode material, CE and WE, was made of GAC.

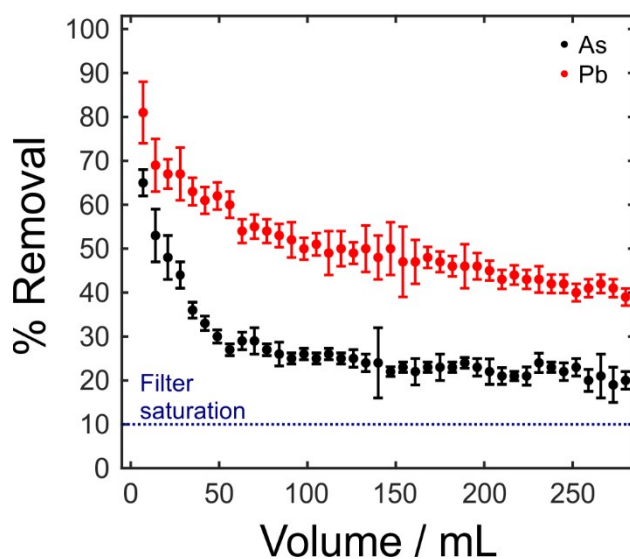


**Figure S2:** Saturation and removal efficiency tests for the different metals using the syringe PoWUFU and applied potential of -1 V vs QRE AgCl of a solution containing 1 ppm of As and Pb in 1M HCl. Each point represents the specific metal concentrations measured by ICP-OES in each 7 mL aliquot passed through the filter. The dotted line represents the saturation of the filter.

### Improving Filtration Using Electrochemistry

In line with electrodeposition in industrial wastewater practices<sup>2</sup>, applying a constant potential with either a potentiostat or external battery during filtration showed significant improvement in removal efficiency (Figures S2, 3A, -1 V), compared to electroless experiments (Figure 3A, Table S1). An increase of 26.5 % for As and 23 % for Pb in the removal efficiency of the device can be seen (Figure 3B).

Whilst encouraging, the removal efficiency reported in Figure 3B was insufficient for practical applications mainly due to the low pH and high chloride concentration.<sup>3-5</sup> Increasing the pH of a solution of deionized water to 5.5 improved the removal efficiency of As and Pb by 32 % and 24 %, respectively (Figures 4, S4). It is also evident that the treatment can be applied directly on tap water without adjusting the pH levels, however further cleaning cycles will be required in order to reduce the metal levels to drinkable levels.

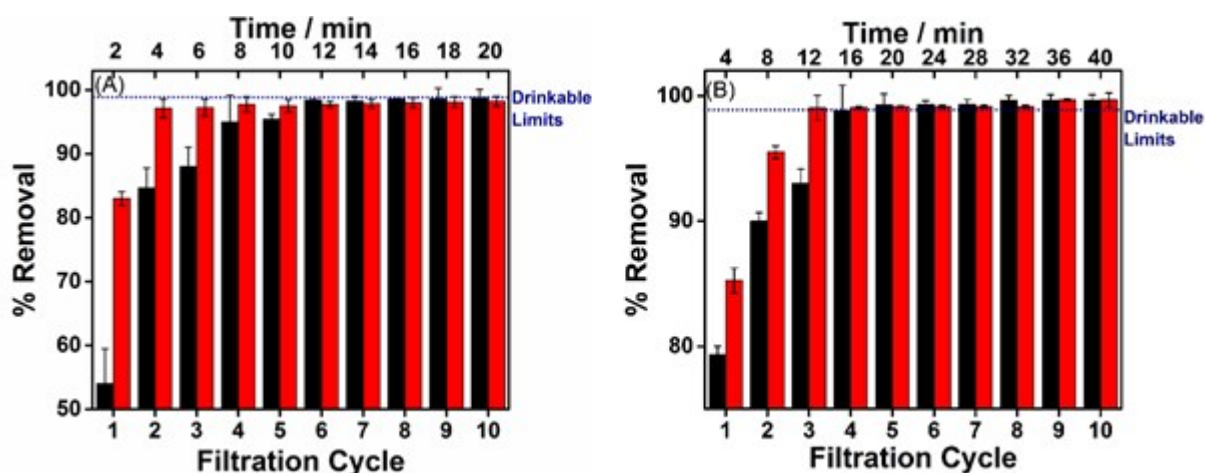


**Figure S3:** Removal efficiency as a function of filtration cycle As (Black) and Pb (Red) using (A) 100 mL and (B) 1 L PoWUFU and tap water (pH 6) spiked with 1 ppm of As and Pb (each) while applying a potential of -1 V vs QRE Ag/AgCl. The confidence level was calculated based on a standard deviation (95%) of 5 repeats.

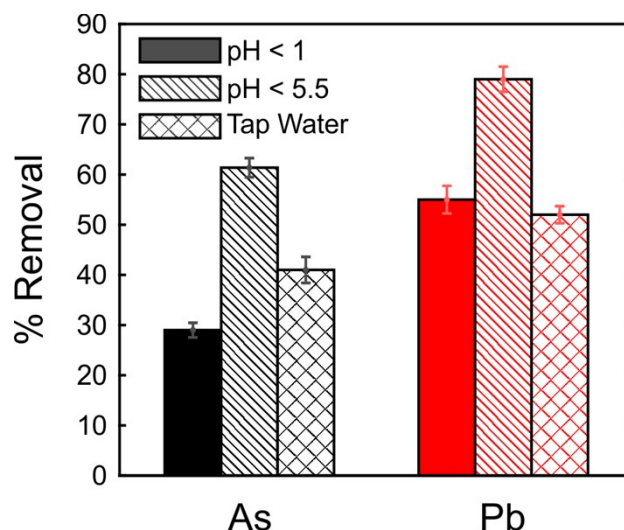


**Figure S4:** Removal efficiency of As and Pb using different solutions while applying a potential of -1 V vs QRE AgCl and a syringe PoWFU. Deionized water at pH<1 (Solid), deionized water at pH 5.5 (Striped) and clean tap water (Cross hatched) all spiked with 1 ppm of As and Pb (See also Figures S5, S6). The confidence level was calculated based on a standard deviation (95%) of 5 repeats.

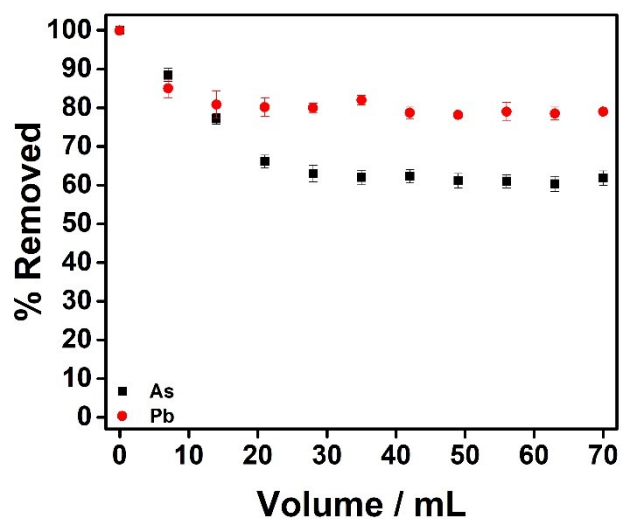


**Figure S5:** Removal efficiency for the different metals using deionized water at pH 5.5 while applying a potential of -1 V vs QRE AgCl using a syringe PoWFU. The confidence level was calculated based on a standard deviation (95%) of 5 repeats.

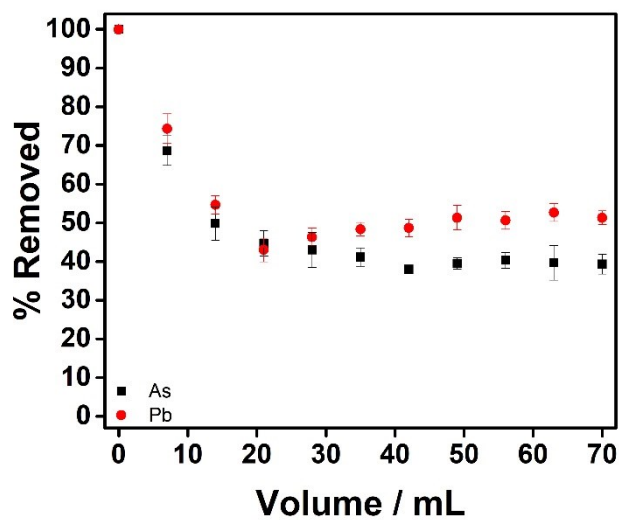


**Figure S6:** Removal efficiency for the different metals using spiked tap water while applying a potential of -1 V vs QRE AgCl using a syringe PoWFUI. The confidence level was calculated based on a standard deviation (95%) of 5 repeats.

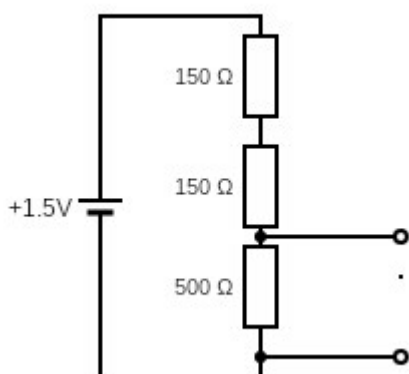


**Figure S7:** Voltage divider circuit design to produce a 0.94 V output from a 1.5 V battery (AA).

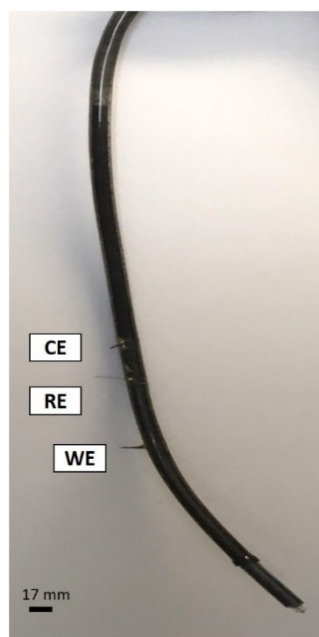


**Figure S8:** The final working PoWFU prototype (Figure 1C 100 mL, Figure S8) was fabricated from a 10 mL syringe and a Tygon tube (I.D. 13 mm O.D. 17 mm, 101 cm total length). The counter electrode (CE) and working electrode (WE) contained 20 g of GAC (each).

### Morphology of GAC

The morphology of the GAC used is exemplified by the following three representative images. The images were obtained by scanning electron microscopy using the secondary electron detector. Three different morphologies were observed, the first of which (presented in Figure S9) is the most common. Area 1 (Figure S10) is relatively smooth and not apparently porous on the scale imaged. Area 2 (Figure S11) represents a porous region with striations in the surface while Area 3 (Figure SX3) appeared smooth but porous.

From the EDX images provided for each representative area, some, seemingly homogeneously distributed impurities appeared, namely S, O and Cl. In addition, across all three areas (EDX images in Figures 1-3) inclusions were observed, comprised of individual elements, specifically Si, Al, Ca, and Fe. The inclusions can be concluded to be either ceramic carbides (e.g. SiC or Fe<sub>3</sub>C), metallic/semi-metallic or some combination of both. As EDX cannot identify oxidation states, further surface analysis would be necessary to distinguish between the two possibilities (elemental vs. carbide) however, a detailed characterization of the surface of the GAC is not the focus of this work.

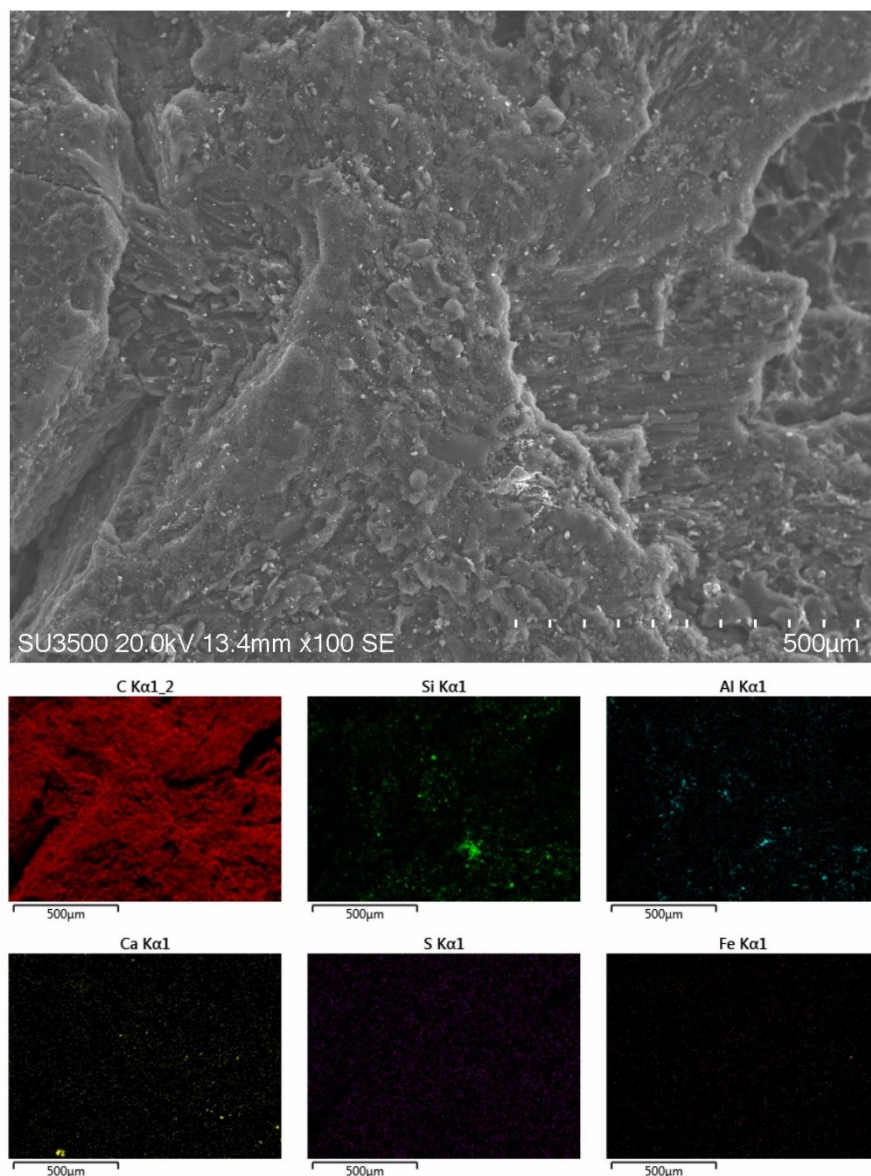


Figure S9: SEM image showing GAC morphology of representative area #1. EDX maps of the same area broken down by detected element.

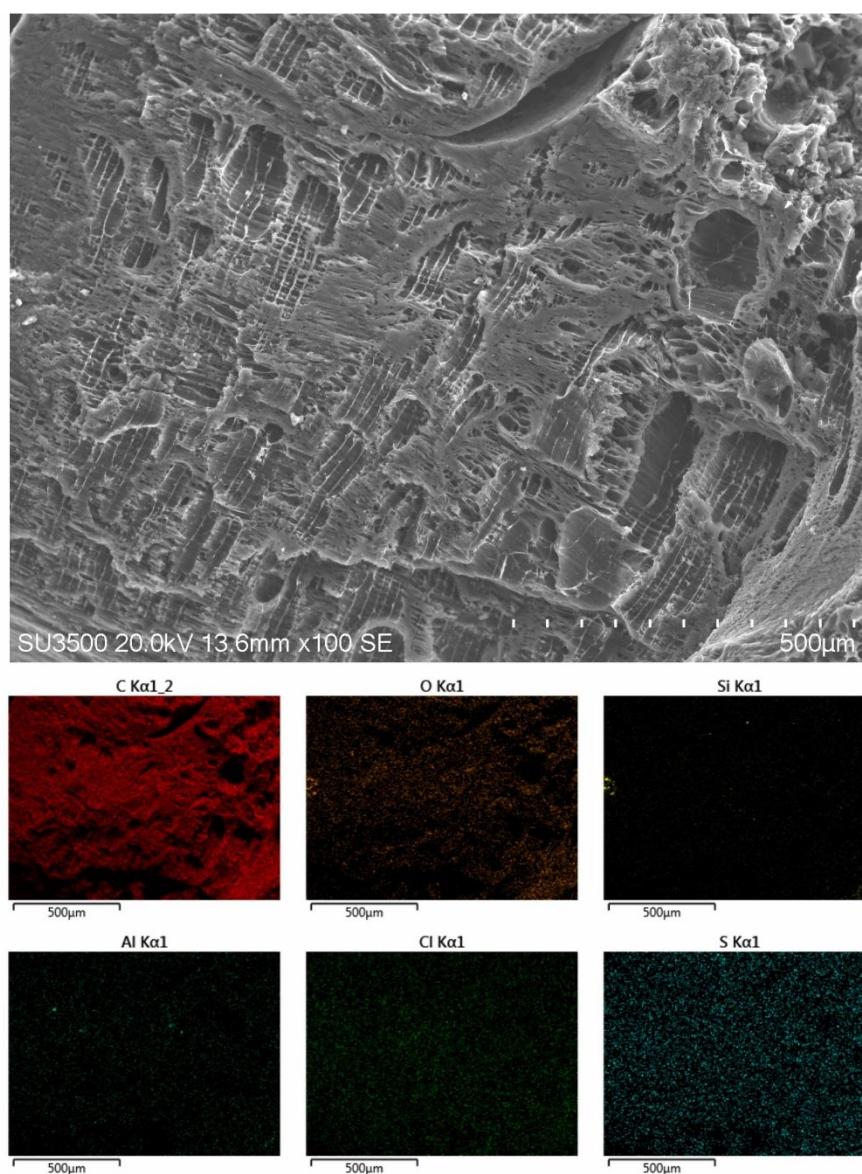


Figure S10: SEM image showing GAC morphology of representative area #2. EDX maps of the same area broken down by detected element.

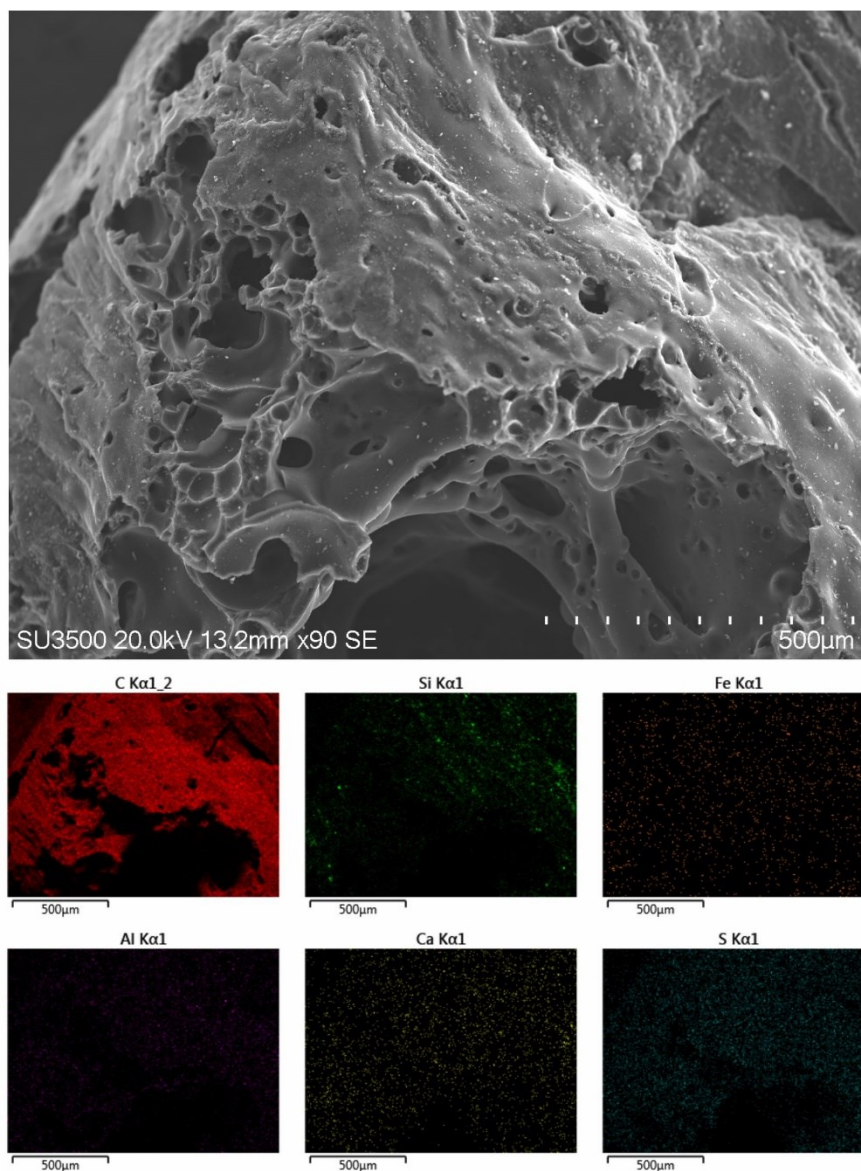


Figure S11: SEM image showing GAC morphology of representative are #3 EDX maps of the same area broken down by detected element.

### Conflicts of interest

There are no conflicts to declare.

### Acknowledgements

The authors are grateful for funding from Natural Sciences and Engineering Research Council of Canada (NSERC) (grant RGPIN/05002-2014).

### References

- 1 A. J. Bard, R. Parsons and J. Jordan, *Standard potentials in aqueous solution*, Marcel Dekker, Inc., New York, NY, United States, 1985.
- 2 H. I. Maarof, W. M. A. W. Daud and M. K. Aroua, *Reviews in Chemical Engineering*, 2017, **33**, 359-386.
- 3 S. Laschi, I. Palchetti and M. Mascini, *Sens. Actuator B-Chem.*, 2006, **114**, 460-465.
- 4 M.A. Barakat, *Arab. J. Chem.*, 2011, **4**, 361-377.
- 5 J. Heffron, M. Marhefke and B. K. Mayer, *Sci. Rep.*, 2016, **6**, 28478.